ESTIMATES OF CELLULAR MECHANICS IN AN ARTERIAL SMOOTH MUSCLE

S. P. DRISKA, D. N. DAMON, AND R. A. MURPHY,
Department of Physiology, University of Virginia School of Medicine, Charlottesville, Virginia 22908 U.S.A.

ABSTRACT Estimates of force generation or shortening obtained from smooth muscle tissues are valid for individual cells only if each cell is contracting homogeneously and if cells anatomically arranged in series are mechanically coupled. These two assumptions were tested and shown to be valid for the pig carotid media under certain conditions. Homogeneity of cellular responses in carotid strips was estimated from the motion of markers on the tissue during K^+-induced isometric contractions. When tissues were stretched to L_0 (the optimum length for force generation), there was little marker movement on stimulation. However, considerable marker movement was observed on stimulation at shorter muscle lengths, reflecting localized shortening or stretching. The mechanical coupling of the very small cells in the media was determined by measuring the dependence of cell length on tissue length. Tissues were fixed with glutaraldehyde during isometric contractions at various tissue lengths (0.4–1.1 × L_0). The fixed tissues were macerated with acid and the lengths of the dispersed cells were measured. Cell lengths were broadly distributed at all muscle lengths. However, the direct proportionality between mean cell length and muscle length (as a fraction of L_0) indicated that cells which are anatomically in series are coupled force-transmitting structures. We conclude that valid estimates of cellular mechanical function in this preparation can be obtained from tissue measurements at lengths greater than about 0.9 L_0.

INTRODUCTION

A number of critical studies on the mechanics of smooth muscle tissue preparations have been made. In general, such preparations exhibit mechanical properties qualitatively resembling striated muscle. The maximum force developed/cross-sectional area of smooth muscle cells (F_0) often equals or may exceed that of skeletal muscle cells (reviewed by Murphy, 1976). The force-generating capacity is striking, as the myosin content of smooth muscle cells is only one-fourth that of skeletal muscle (Murphy et al., 1977; Murphy et al., 1974). However, the applicability of mechanical measurements on tissues to smooth muscle cells is conjectural. First, all such studies have assumed that cellular activation and contractile output are homogeneous in the complex tissues. Second, the mechanical arrangement of cells within the tissues is un-

---

Some preliminary data on cell length as a function of tissue length were reported at the Heidelberg Symposium on Smooth Muscle (Murphy et al., 1977).

Dr. Driska was the recipient of a National Institutes of Health Post-Doctoral Fellowship, F32-HL 05180.

known. One explanation for the high tissue force-generating capacity is that the anatomical cross section underestimates the number of smooth muscle cells developing force in parallel, and overestimates cellular force generation (Bader, 1963; Burton, 1954; Gabella, 1976; Huxley, 1957; Murphy, 1976).

These uncertainties cannot be resolved by direct measurements, as viable single cell preparations have not been obtained from mammalian smooth muscles. However, indirect approaches involving tissue measurements can provide the desired information. If tissue properties directly reflect cellular properties (mechanically this means that force is transmitted between cells anatomically arranged in series [Murphy, 1976]), then two predictions can be made. (*a*) In a tissue of constant cross section stretched to its optimum length for force development (L_0), active force depends only on the cross-sectional area and not on the absolute length of the tissue segment isolated for study. (*b*) Cell length will be directly proportional to tissue length over the working range of the tissue. Evidence supporting the first of these predictions was found for the pig carotid artery (Driska and Murphy, 1978). Experiments testing the second prediction are described in this report, together with direct observations on regional movement during isometric contractions in a smooth muscle tissue. The results suggest that estimates of contractile function obtained from tissues at L_0 can be extrapolated to the behavior of individual cells in the smooth muscle of the pig carotid artery.

METHODS

Smooth Muscle Strips

The collection of pig carotid arteries, preparation of intima-media strips, and determination of their length-tension relationships have been described (Herlihy and Murphy, 1973). The smooth muscle cells were aligned in parallel in the axis of the strip. Cross-sectional areas were obtained as mass (density × length), a calculation which agrees with direct optical determination (Herlihy and Murphy, 1973). The anatomical extracellular space, determined from electron micrographs, was 40% (Herlihy and Murphy, 1973), whereas the sucrose space was 37% (this study).

Solutions

The physiological salt solution (PSS) had the following millimolar composition: NaCl, 117.8; KCl, 6.0; $NaHCO_3$, 24.3; NaH_2PO_4, 1.2; Na_2-ethylenediaminetetraacetic acid (EDTA), 0.027; $CaCl_2$, 1.6; $MgSO_4$, 1.2; and *d*-glucose, 5.6. The solution was bubbled continuously with 95% O_2, 5% CO_2, giving a pH of 7.45 at 37°C. High-potassium PSS (K^+-PSS) was identical except for an equimolar substitution of KCl for NaCl. Some strips were rendered atonic before fixation by bathing them for 30–180 min in (*a*) K^+-PSS lacking Mg^{++} and Ca^{++} with 1 mM EDTA added, or (*b*) glucose-free K^+-PSS plus 10 mM NaN_3 bubbled with 95% N_2, 5% CO_2. Active force in these muscle strips decayed to zero and there was no redevelopment of force after a quick release.

Fixation and Maceration

Strips were stimulated with K^+-PSS and, when force reached a maximum, the bathing solution was replaced with an isosmotic fixative containing: glutaraldehyde (Electron Microscopy Sci-

ences, Fort Washington, Pa.), 2%; sucrose, 0.1 M; sodium cacodylate-HCl buffer (pH 7.4), 0.1 M (Arborgh et al., 1976). Addition of the fixative generally caused a slight increase in force. Strips were fixed for 10 min at 37°C, followed by 12–18 h at 25°C. After fixation, the strips were cut from the clips, blotted lightly, and weighed. The strips were then successively macerated for 30 min in 0.6, 1, 2, 10, 20 and 25% HNO_3 (Uvelius, 1976), followed by 4 days in 30% HNO_3. The tissues were then placed in 5 ml of 0.2 M Tris as the free base overnight. The pH was adjusted to 7.4 with magnetic stirring. This produced some disruption of the tissue. The suspension was rinsed into centrifuge tubes with 5 ml H_2O, allowed to stand for 1 hr, and centrifuged for 10 min at 3,000 *g*. The sedimented cells were suspended in 0.5 ml 50% glycerol, 0.1 M Tris-HCl (pH 7.40) by vigorously agitating for 10 s with a Vortex mixer (Scientific Industries, Inc., Bohemia, N.Y.).

Measurement of Cell Lengths

10 μl of each cell suspension was mixed with 10 μl of 0.05% toluidine blue in 2.4% Na_2CO_3 on a microscope slide and a cover-glass was added. Cell lengths were measured at 100 or 400 × magnification with a microscope equipped with a filar ocular micrometer. Cells selected for measurement had (*a*) unbroken ends, (*b*) clearly discernable borders, if still attached to another cell, and (*c*) were straight or bent in a shape whose length could be measured accurately.

Uniformity of Response Studies

Smooth muscle strips were horizontally mounted in a chamber (45 × 10 × 10 mm) constructed on a Lucite platter. Strip ends were connected by stainless steel clips and rods to a micrometer drive and a Grass FT.03C force transducer mounted on the Lucite platter (Grass Instrument Co., Quincy, Mass.). Total system compliance was <10 μm/g (10^{-3} m/N). The transducer output was displayed on a Gould 260 recorder (Gould, Inc., Instrument Systems Div., Cleveland, Ohio). The Lucite platter was attached to the stage of a Leitz Labolux II microscope (E. Leitz, Inc., Rockleigh, N.J.) and illuminated by a xenon source (Fig. 1).

Strips mounted in the well of the chamber were superfused with PSS or K^+-PSS at a flow rate of 5–7 ml/min at 37°C. When strips were mounted and stretched they exhibited the slow con-

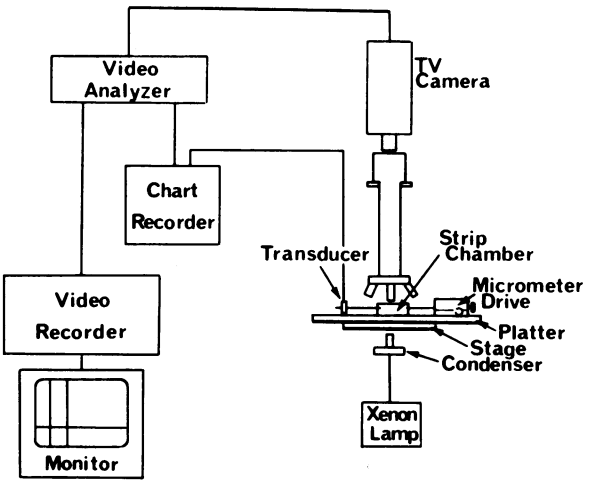

FIGURE 1 Apparatus for high resolution measurement of marker positions. Details are given in the Methods.

traction and relaxation typical of good preparations (Herlihy and Murphy, 1973). After the strips were equilibrated, glass micropipettes (tip diameter of 10–15 μm) filled with a 3-μm Millipore-filtered (Millipore Corp., Bedford, Mass.) carbon particle suspension (Pelikan black special ink, Günther-Wagner, Hanover, W. Germany) were positioned using a Leitz micromanipulator. Particle movement from the pipette tips confirmed solution flow over the surface of the strip. When the pipette tip just touched the surface of the tissue, some of the carbon particles adhered in an irregular localized area identifiable as a single spot for low resolution measurements or as a distinctive series of closely spaced markers at high magnification. The shapes of individual markers were reversibly distorted with stretch of the tissue, but the adhesion of the carbon particles was strong enough to preserve the clearly recognizable character of individual marks. Markers were placed in close proximity to the clip for high magnification examination, and five to seven marks (depending on strip length) were distributed along the entire strip for low magnification study. The strip was then stretched to approximately 1.1 L_0 for length-tension determination, and subjected to cycles of K^+ stimulation and relaxation until a consistent active force was developed. Marker positions were referenced to the vernier scale on the microscope stage drive when centered in an eyepiece equipped with cross-hairs. This system allowed spots along the strip to be located ± 50 μm at 100 $\times$ magnification. Spot locations were plotted at different muscle length in "resting" (unstimulated) and isometrically contracted K^+-activated tissues.

Measurement of the marker positions at high magnification was made with a closed-circuit television system consisting of a Cohu 3200 camera with a silicon diode array photodetector (Cohu Inc., San Diego, Calif.), Colorado Video analyzer 321 (Colorado Video, Inc., Boulder, Colo.) Sony EV-210 Videocorder (Sony Corp. of America, Long Island City, N.Y.), and a Conrac high resolution monitor (Conrac Corp., New York) (Fig. 1). For each muscle length, a view of one end of the tissue and the clip was videotaped during a quick release and on subsequent stimulation (the rationale for this protocol is described in Results). Marker distance to the clip was measured after the videotape was played back and stopped on a frame following the quick-release. This permitted measurement of transient movement by means of a pair of movable monitor lines generated by the Colorado video analyzer (Gorczynski, 1976). One of these lines was positioned on the clip edge and the other on the marker feature. A DC voltage proportional to the distance separating the lines was obtained. When calibrated against a stage micrometer, measurements with a precision of ± 5 μm were obtained. Since spot measurements were made relative to the end of the clip, system compliance could result in slight marker movement. In a worst case analysis, this would produce an error or $<3\%$ in the distance from the clip to the marker during active force development.

Statistical Analysis of Cell Length Data

Because we found substantial variation in cell lengths at any muscle length, we wished to test whether the means were statistically different. The t test was not strictly appropriate because cell lengths were not normally distributed. This necessitated a fairly elaborate statistical analysis.

Cell lengths were analyzed with the aid of three computer programs. HIST was used to plot histograms, compute means, standard deviations, and coefficients of dispersion, skewness, and kurtosis, as well as the expected coefficients of skewness and kurtosis for nine model distributions. NORFIT was used to perform a chi-square test on the fit of the data to a normal distribution. GAMFIT was used to compute maximum likelihood estimates of α and β for the data fitted to a gamma distribution (which best described the data; see Results), perform a chi-square test on the fit of the data to the model, and compute the probability that the data came from that gamma model. (The probability density function for a gamma distribution is given by $f(x) = ((x/\beta)^{\alpha-1}\exp(-x/\beta))/(\beta\Gamma(\alpha))$, where the product of α and β is the mean

and $\Gamma(\alpha)$ is equal to $(\alpha - 1)!$. Gamma distributions are always positively skewed and can assume a variety of shapes, depending on the value of α, the shape parameter [Bury, 1975].) The good fit of the data to gamma distributions allowed us to use the following technique to compare mean cell lengths at different tissue lengths (Gross and Clark, 1975). The Neyman-Pearson test statistic, λ, is equal to the product of the probabilities of observing each datum under the null hypothesis, divided by the product of the probabilities of observing each datum under the alternate hypothesis. When the null hypothesis is true, this fraction will be large. To compare two gamma distributions, the data were pooled and a common value of α was obtained with GAMFIT. The null hypothesis tested was that $\beta_1 = \beta_2 = \beta$, i.e., that the distributions were the same, whereas the alternate hypothesis was that $\beta_1 \neq \beta_2$. For two gamma distributions with a common value of α, the Neyman-Pearson test statistic reduces to $\lambda = [(\bar{x}_1)^m(\bar{x}_2)^n/(\bar{x})^{m+n}]^\alpha$, where m and n are the number of data points in samples 1 and 2, $\bar{x}_1$ and $\bar{x}_2$ are the respective means, and $\bar{x}$ is the mean of the pooled data. For large values of m and n, the variable, $\Lambda = -2 \ln \lambda$, is chi-square distributed with 1 df. A value of Λ for each comparison (0.4 vs. 0.6 L_0, 0.6 vs. 0.8 L_0, etc.) was computed. The probability of obtaining such large values of Λ when the null hypothesis is true is equal to the probability that $\chi_1^2 > \Lambda$. Because of a chi-square distribution with 1 df is the square of a standard normal distribution, the probability that $\chi_1^2 > \Lambda$ is equal to the probability that $|Z| > \sqrt{\Lambda}$, or twice the probability that $Z > \sqrt{\Lambda}$, where Z is the standard normal variable: $P(\chi_1^2 > \Lambda) = P(|Z| > \sqrt{\Lambda}) = 2\,P(Z > \sqrt{\Lambda})$. The descriptive levels (or P values) were then computed from the standard normal distribution.

RESULTS

Homogeneity of Response: Low Resolution Experiments

We sought to determine if cellular activation and contraction were uniform by looking for localized shortening or lengthening during contraction of a tissue at a fixed overall length. We reasoned that partially activated cells within a tissue would be stretched by fully activated cells in series with them. This would produce observable movements during isometric force development. Two series of experiments were done. In the first, the entire length of five muscle strips was studied at different degrees of stretch, and the positions of the markers were measured at 100 × magnification (using the calibrated stage drive of the microscope), both in a resting condition (with a low, but unknown level of tone), and then during K^+ stimulation.

Fig. 2 shows a typical example from this series of experiments. At short muscle lengths there was considerable movement of the markers with stimulation. At lengths near L_0, however, there was little movement. Since marker movement at short lengths was to the left (Fig. 2), it appears that this was predominantly due to lengthening of a small region near the right end of the tissue. Some tissues exhibited marker movement in both directions at any given length. The direction of movement of the markers on activation was not always toward the center of the strip, as might be expected if clip damage were the sole cause. Another property of the muscle strip demonstrated in Fig. 2 is the uniformity of its elastic properties. In a homogeneous substance, one would observe a direct proportionality between marker position and stretch of the material. In the range of muscle lengths studied, such a plot of marker position vs.

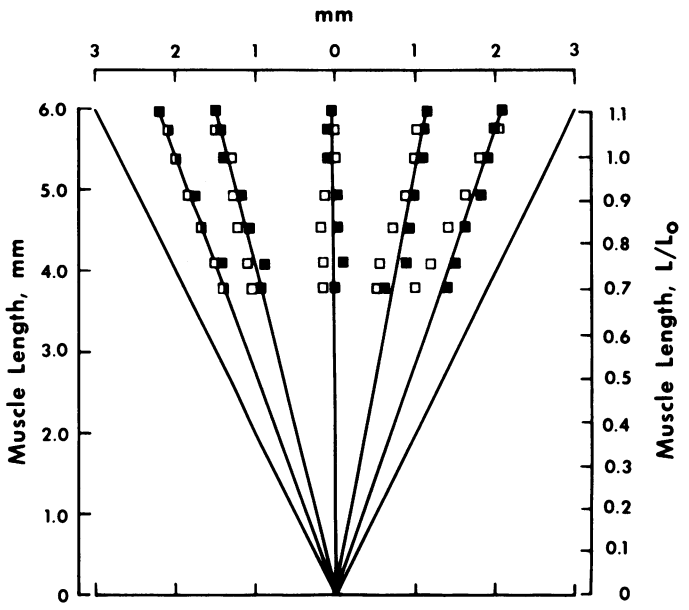

FIGURE 2 Marker positions at different muscle lengths before (■) and after (□) K^+ stimulation. Positions of markers in one muscle strip at various lengths are plotted on the abscissa, referenced to the center of the muscle strip. The muscle length is plotted on the ordinate. Thus, each horizontal row of symbols represents marker positions at a fixed tissue length. Lines are drawn from the origin to marker positions under maximum stretch, showing predicted behavior of a uniformly elastic substance. The lines at left and right indicate the ends of the tissue in the clips.

strip length extrapolates reasonably well to zero length. This measurement gives an index of the uniformity of stretch along the length of the tissue.

High Resolution Experiments and Quick Release

The first set of experiments gave a general picture of the behavior of the tissue, but suffered from relatively low resolution and the presence of some degree of tone in the unstimulated tissue. Consequently, marker position in the resting tissue may not accurately indicate the passive equilibrium of tissue elements. Passive elastic forces are best determined in this tissue immediately after a rapid release (Herlihy and Murphy, 1973). The basis of this procedure is that the elastic elements equilibrate rapidly after a step shortening, and true passive properties can be estimated before the slow redevelopment of tone by the partially activated contractile system ensues (Jewell and Wilkie, 1958). In the second series of experiments, a small area near the end of each of six muscle strips was studied under higher magnification (370 ×) and the marker positions were measured electronically on playback of a videotape. With this system, it was possible to measure the positions of the markers within 500 ms after a quick release and refocusing. This minimized the effect of tone on marker position and changes could be monitored continuously during subsequent K^+ stimulation.

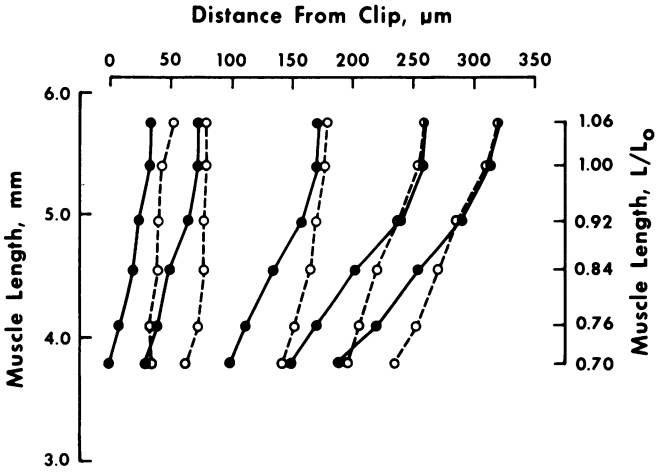

FIGURE 3 High resolution marker positions (abscissa) in the region of the muscle clip in one muscle strip at different muscle lengths (ordinate). (•) Position after quick release to the indicated muscle length; (○) marker position after development of isometric tension in response to K^+. Lines connect the positions of a given marker at different muscle lengths.

Fig. 3 shows the results of one of these experiments. The markers were deposited on the adventitial side of the media and the strip length was varied between 0.70 and 1.11 × L_0. Observations at shorter lengths were not possible because the horizontally mounted strip sagged out of the plane of focus and made measurements unreliable. Two features should be noted: (*a*) movement on activation is toward the center of the muscle strip, and (*b*) the amount of movement observed at lengths near L_0 is small, but

TABLE I
MEAN MARKER MOVEMENT IN HIGH RESOLUTION EXPERIMENT

Normalized length	Mean marker movement ±SEM	*n*
	μm	
0.601–0.700 L_0	21.8 ± 8.0	5
0.701–0.800 L_0	29.0 ± 3.7	23
0.801–0.900 L_0	17.8 ± 3.6	16
0.901–1.000 L_0	15.4 ± 1.7	48
1.001–1.100 L_0	12.0 ± 1.6	28

Marker movement is defined as the difference between the marker positions after quick release and after K^+ activation. Data were collected within 700 μm from the muscle clip on the adventitial surface of four muscle strips. Each strip had three to five markers and was studied at various muscle lengths. Measurements were grouped according to the normalized muscle length, L/L_0. The mean value of L_0 was 8.11 mm. In two additional experiments the markers were placed on the intimal surface of the tissue. The pattern of marker movements was more variable (see text) and these results are not included in this tabulation.

it increases at shorter muscle lengths. In this experiment, the maximum movement observed was about 50 μm at 0.70 L_0 and 10 μm at L_0. If the 50-μm movement were uniformly dissipated along the strip (so that there was no movement at its center), it would amount to ~2.5% shortening. Table I summarizes the results of the high resolution observations at the ends of the muscle strips.

In this preparation the series elasticity has been characterized (Herlihy and Murphy, 1974) and an extension of 0.072 L_0 was demonstrated during maximum force develop-

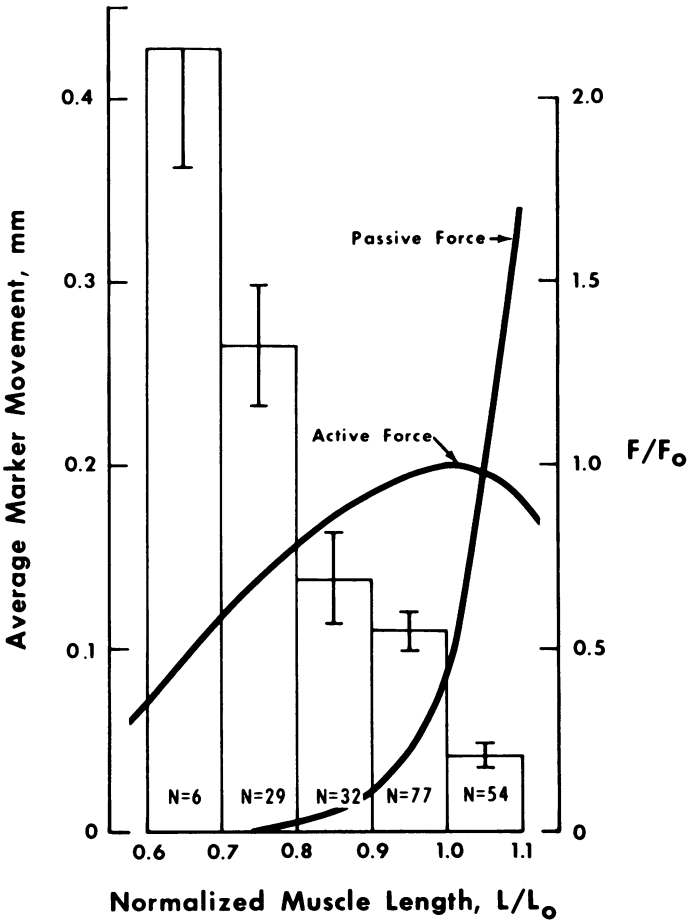

FIGURE 4 Average marker movement in low resolution experiments. Data are averages ±SEM from measurement on five muscle strips, each having five to seven markers along the entire length of the adventitial surface of the media. Each muscle was studied at several lengths. Movement is the difference in marker position between unstimulated and stimulated muscles. Experiments were grouped according to normalized muscle length, i.e., muscle length/L_0. Thus, N is the total number of markers observed at all normalized lengths in the interval. Active and passive force-length curves for this preparation have been superimposed for comparison, with force being normalized to F_0, the maximum active force developed. Average marker movement in each of the intervals is significantly different ($P < 0.001$, t test) from that in the 1.0–1.1 L_0 interval.

ment at L_0. The mean movement seen at L_0 is ~ 15 μm, or 0.0019 L_0 (Table I). If the measured series elasticity at L_0 were due entirely to clip damage, one would expect a movement of 0.036 L_0 at each end, or ~ 292 μm. Thus, clip damage seems to account for only a small percentage ($\sim 5\%$) of the series elastic component (SEC) extention during a maximum contraction at L_0. The properties of the SEC at shorter lengths in this preparation are not known.

Not all experiments exhibited the uniformity in marker movements seen in Fig. 3, particularly if the markers were deposited on the smooth intimal surface of the preparation. In some cases markers moved toward the clip, which is not readily explainable if there is appreciable clip damage. Movement of markers deposited on the endothelial cells of the intima may be a poor indicator of motion in the media, however, and all measurements summarized in Table I were made on the adventitial surface of the media. The one common finding of all experiments was greater movement at short muscle lengths. This could be the result of regional length-dependent effects on activation processes, or reflect length-dependent structural rearrangements limiting the extent of localized shortening or stretching. The latter possibility was examined by comparing mean marker movements (from the low resolution experiments) at different tissue lengths with the forces at those lengths. Fig. 4 shows mean marker movements superimposed on the length-tension curve of this preparation (Herlihy and Murphy, 1973). It is clear from Fig. 4 that marker movement is not simply proportional to active force alone, because maximum active force does not result in maximum movement. Furthermore, a given value of active force does not define a unique value of marker movement, i.e., equal active forces on the ascending and descending limbs of the length-tension curve result in different marker movements. Fig. 4 also shows that marker movement decreases as passive force increases. From this, we infer that increased passive force could have some role in limiting marker movement.

Mean Cell Length as a Function of Tissue Length

If cells anatomically in series are coupled force-transmitting structures, stretching the tissue will cause cell length to change so that cell length will be directly proportional to normalized muscle length (e.g. a 10% stretch of the tissue will increase cell length 10%). If, however, cells anatomically in series function in parallel (e.g. by transmitting force exclusively to a connective tissue network), then a given tissue stretch will result in a proportionally greater increase in cell length (e.g. a 10% increase in tissue length might result in a 20% increase in cell length). To determine the dependence of cell length on tissue length, three sets of strips were fixed with glutaraldehyde during K^+ contractures at muscle lengths of 0.6, 0.8, 1.0, and 1.1 $\times$ L_0, and two muscle strips were fixed at 0.4 L_0. After maceration, the lengths of 50 dispersed cells were measured from each tissue. Fig. 5A shows the mean cell lengths at each muscle length, ± 1 SEM. The dotted line is drawn through the mean cell length at L_0 to the origin and predicts the mean cell length at any muscle length if the cells are linked in series (as in the tissue model in panel C). The dashed line indicates cell lengths expected in a tissue model

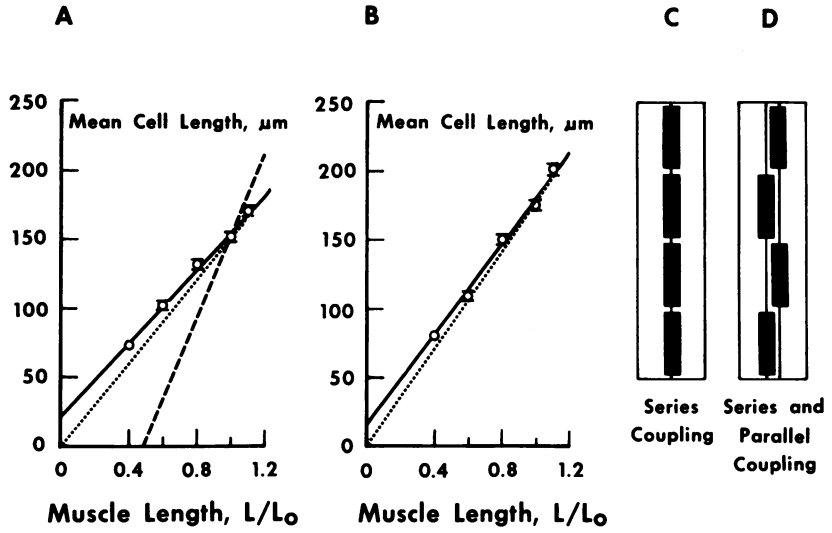

FIGURE 5 Dependence of cell length on tissue length. (A) Plot of mean cell length vs. normalized muscle length. Points represent means of 100 (muscle length = 0.4 L_0) or 150 (all other muscle lengths) cells ±1 SEM. Lines drawn show: least squares regression of data (solid lines); behavior predicted by series model (dotted lines); behavior predicted by a model where there is some parallel coupling of cells anatomically in series (dashed line). (B) Same as A except that cell lengths are corrected for differential shrinkage. (C and D) Two schematic tissue models of equal volume containing four identical cells. The thin lines indicate force transmission by relatively inextensible structures. In C, the series model, the cells are coupled force-transmitting structures and cell length is directly proportional to tissue length. In D, the model with both series and parallel coupling, some cells function in parallel even though they are anatomically in series, enabling this tissue to develop twice as much force. A consequence of this arrangement is that cells have to shorten twice as much to cause a given shortening of the tissue.

such as that depicted in panel D, which is one of many ways cells could be coupled in parallel to allow the tissue to develop twice as much force per cross-sectional area as the cell. Any parallel coupling would be detected if the data fit a line with a steeper slope than that of the series line. Least squares analysis of the data results in a regression line with a positive y-intercept and a slope less than the series line. The slope of the line for the series model is, however, within the 95% confidence interval for the regression line fitted to the experimental data.

Fixation did not affect tissue length but maceration of fixed tissues in acid produced longitudinal shrinkage, which was partially reversible on neutralization. If cell lengths were reduced similarly, it would affect the interpretation of the data. The extent to which cell shrinkage was reversible was estimated by measuring the lengths of fixed tissues before and during maceration in acid and, finally, when the tissue was suspended in 50% glycerol, 0.1 M Tris-HCl, pH 7.40. Final lengths at pH 7.4 were 0.85–0.93 times the in vitro lengths before fixation, with shrinkage being more reversible in shortened tissues. Mean cell lengths at each muscle length were divided by the appropriate fraction to correct for shrinkage and plotted in Fig. 5B. The regression line

in Fig. 5B is in better agreement with the behavior predicted by the series model. It is important to note that it still does not exceed the slope of the line for the series model, nor is it significantly different at the 95% level. Thus, we feel that variable shrinkage does not compromise our interpretation of the data illustrated in Fig. 5 as evidence for the series model.

While the mean cell length was a linear function of tissue length (r = 0.99) (Fig. 5), the distribution of cell lengths at each tissue length was broad (Fig. 6). The data were analyzed to determine if the mean cell length at a given muscle length was significantly different from the mean cell length at other muscle lengths. The statistical analysis showed a highly significant difference between all mean values (descriptive levels of <0.00012) in paired comparisons of adjacent muscle lengths. The total descriptive level for the experiment (i.e. the probability that differences in mean cell length are not

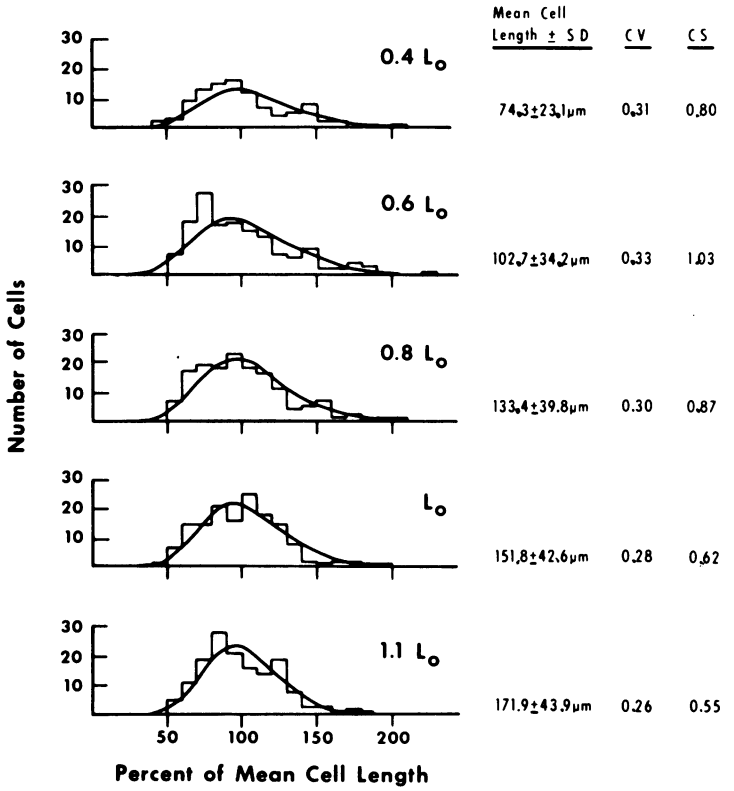

FIGURE 6 Normalized histograms of cell length in muscles contracting isometrically at different lengths. The "bin width" corresponds to 10% of the mean cell length at that particular muscle length to facilitate comparisons of distributions with different means. The smooth curves superimposed on the histograms are the maximum likelihood gamma distributions computed for the data. Also shown for each muscle length are the mean and standard deviation, the coefficients of variation (CV), and the coefficients of skewness (CS). Positive coefficients of skewness indicate skewing to longer lengths. Number of cells counted was 100 at 0.4 L_0, and 150 at all other muscle lengths.

real) is approximately equal to the sum of the descriptive levels of the paired comparisons, or ~0.00020.

Histograms of Cell Length

We were interested in the uniformity of cell length in the tissue since a high degree of uniformity would suggest that the cell is a precisely repeating subunit, much like the sarcomere in a skeletal fiber. Cell lengths from tissues fixed during isometric contractions at different muscle lengths are shown in Fig. 6 as histograms. The histograms in Fig. 6 show large variations of cell length within a tissue, unlike skeletal muscle (Close, 1972). The mean length, standard deviation, coefficient of variation, and coefficient of skewness are shown in Fig. 6. The coefficient of variation is a convenient quantitative expression for the nonuniformity of cell lengths.

It is apparent that the distribution of cell lengths is similar at all lengths, although there is a trend toward a relatively wider distribution of cell lengths in shortened tissues (i.e., greater coefficients of variation). The data were analyzed by a computer program which performed routine statistical calculations on the sample data, including coefficients of skewness and kurtosis. It then used these calculations to produce coefficients of skewness and kurtosis to be expected from these sample data if they were derived from a population distributed according to the following models: normal, log-normal, exponential, double exponential, uniform, gamma, Weibull, and extreme value type I. At every muscle length a gamma distribution appeared to be most likely. Data analysis would be simplified if cell lengths were normally distributed, and this was examined by a chi-square test. The descriptive levels for the normal model in Table II were computed under the null hypothesis that the data came from a normal distribution. A descriptive level >0.10 indicates a good fit and was observed in only one case. Thus, the null hypothesis that cell lengths are normally distributed was rejected. Table II also shows descriptive levels obtained when a chi-square test on the fit of the data

TABLE II

DESCRIPTIVE LEVELS (*P* VALUES) FOR FIT OF CELL LENGTHS TO MODEL DISTRIBUTIONS

Muscle length (L/L_0)	Model distribution	
	Normal	Gamma
0.4	0.013911	0.244087
0.6	0.000037	0.144250
0.8	0.033520	0.468279
1.0	0.309667	0.122081
1.1	0.077134	0.256413

The null hypothesis is that the population has the distribution being tested. The chi-square value of the sample is then computed, and the descriptive level (*P* value) is the probability of a chi-square value this large or larger when the null hypothesis is true.

to a gamma distribution was performed. In this case, the higher descriptive levels indicate that cell lengths were consistent with a gamma distribution. While the physiological meaning of a gamma distribution is not known, the good fit of the data was helpful because it permitted the use of parametric analysis (see Methods) for a critical statistical test of differences in mean cell length.

DISCUSSION

Homogeneity of Response and Implications for Smooth Muscle Mechanics

Our analysis of localized movements during isometric contractions assumes that superficial markers are accurate indicators of movement throughout the media. Observation of deeper tissue layers was not feasible due to the thickness of the preparation. Consequently, the data are best regarded as an index of overall tissue behavior which cannot be quantitatively interpreted at the cellular level. Substantial localized shortening on isometric stimulation was only observed at short muscle lengths. This could arise from (*a*) nonuniform activation at lengths below L_0, or (*b*) nonuniform activation and contraction at all lengths, masked at L_0 due to the increased passive forces limiting localized shortening. Although differential activation at optimum tissue lengths cannot be ruled out by these experiments, the data suggest that the connective tissue network plays an important role (Fig. 4). By bearing loads imposed by stretch and by limiting movement within the media, the passive elements might contribute to cell length homogeneity and a homogeneous stress distribution throughout the tissue. However, this uncertainty does not detract from the fact that the observed marker movements at lengths near L_0 were small enough that they should not compromise estimates of force generation. An alternative interpretation is possible if the markers were attached only to connective tissue elements, and if these elements are not involved in active force transmission. Cell movement at short lengths and low passive forces might be reflected in marker movement whereas cell shortening at long lengths and high passive forces would not. This possibility cannot be ruled out, but seems unlikely in view of the evidence for links between smooth muscle cells and connective tissue (Gabella, 1976; Meiss, 1978).

Cell Length as a Function of Tissue Length

Even though the conditions used to release cells from the fixed tissue were harsh, suspensions of dispersed cells were obtained with careful handling. The ends of broken cells were obvious when compared to smoothly tapering ends of intact cells. The mean length of smooth muscle cells in the pig carotid artery at the optimum tissue length corrected for shrinkage was 176.5 ± 4.1 μm, and this value increased or decreased with tissue length as predicted by the series model within experimental error. Furthermore, the series model can explain active force development at $0.4\ L_0$, whereas models which use parallel linkages to gain even a modest 2:1 force advantage cannot (Fig. 5). Similar data collected by Uvelius (1976) for the rabbit urinary bladder, Cooke and Fay (1972) for guinea pig *Taenia coli,* and Halpern et al. (1978) on small rat mesenteric arteries

gave similar results and suggest that the series model may be valid for other smooth muscle tissues.

Cell Length Histograms

The two salient features of the histograms in Fig. 6 are their broadness and skewing to longer lengths. It is conceivable that gross variations in cellular shrinkage during maceration are responsible for the variation in cell length. However, we think it more likely that a shrinkage artifact would be a constant fraction of cell length and not contribute to the shape of the distribution, per se. Undetected breakage of cells could cause skewing, but it would be skewing to shorter lengths and is therefore unlikely. A small population of parallel linked cells would cause progressive skewing to shorter cell lengths with tissue shortening. Geometrical considerations can explain most of the skewing and some of the variation in cell lengths in this preparation. If cells were all the same length in a ring of circular smooth muscle at L_0, with inside, outside, and mean radii of r_i, r_o, and r_m, the difference between the mean and both the inner and outer circumferences is $\pi(r_o - r_i)$. Dividing by the mean circumference gives the fractional difference $(r_o - r_i)/(r_o + r_i)$. With some of the thicker strips used in this study, representative values of r_o and r_i are 2.5 and 2.0 mm, resulting in a fractional difference of 0.11. When such a ring is straightened to form a rectangular solid, the intimal side of the strip may be stretched up to 11% more than the mean, whereas cells on the adventitial side may be 11% shorter than those in the layer corresponding to r_m. Comparable increases in the coefficient of variation of cell length would be expected. In such a ring, there are more cells in the layers from r_o to r_m than from r_m to r_i due to the increased circumference. This inequality in the number of cells at each radius could be responsible for the skewing to longer cell lengths observed when such a ring is opened and straightened. This was shown in one experiment where a segment of carotid artery was threaded on a 5-mm diameter glass rod and fixed as an intact cylinder. The histogram of cell lengths was slightly skewed to shorter lengths (coefficient of skewness = -0.43). The mean cell length corresponded to $\sim 0.66\ L_0$ and the coefficient of variation was less (0.18), but still appreciable.

Finally, we considered the possibility that the variations in cell length were due to variations in activation rather than intrinsic cell length. Cell lengths from atonic or metabolically poisoned strips at L_0 had coefficients of variation of ~ 0.25, similar to the value found with K^+-stimulated tissues. Thus, we concluded that the skewing of histograms might be an artifact but, nevertheless, major differences in length normally exist in arterial smooth muscle cells *in situ*. Slightly lower coefficients of variation (0.16–0.21) can be computed from studies on guinea pig *Taenia coli* (Cooke and Fay, 1972) and rabbit urinary bladder (Uvelius, 1976), where tissue preparation involves little geometric distortion.

Estimates of Cellular Mechanical Properties from Tissue Measurements

On the basis of this and a previous study (Driska and Murphy, 1978), we are confident that the series model adequately describes the mechanical linkages between cells in the axis of force transmission in the pig carotid preparation. This indicates that force

per cross-sectional area of cells within a tissue, or shortening velocity of a tissue expressed as L_o per second give data descriptive of the individual smooth muscle cell. Halpern et al. (1978) reached similar conclusions from measurements on intact segments of small mesenteric arteries where small (up to 12%) changes in internal circumference caused directly proportional changes in the distance between intracellular features. Studies on single cell preparations from amphibian visceral smooth muscle support this argument. Fay (1977) reported that single cells from *Bufo marinus* stomach could develop $\sim 3 \times 10^5$ N/m^2 active force, a figure very close to F_0 for visceral smooth muscle tissue (Murphy, 1976). In addition to this, maximum shortening velocities of intact (Bagby, 1974; Fay and Singer, 1977) and permeable (Small, 1977) single cell preparations from *Bufo marinus* and guinea pig *Taenia coli* are close to what is observed in many intact smooth muscle tissues (Murphy, 1976).

It has recently been suggested (Gabella, 1976) that high force development in guinea pig *Taenia coli* might be due to a complex tissue structure. This suggestion was based on the observation that some myofilaments appear to be attached at the lateral surfaces of the cell to extracellular connective tissue. With such an arrangement, cells or portions of cells could be functionally in parallel although anatomically in series, thereby providing a mechanical advantage. However, a consequence of parallel linkage of series aligned elements is that cell length changes will be proportionally greater than tissue length changes. Therefore, if the model proposed by Gabella (1976) were correct for pig carotid, it should have been detected by the experiments reported here (Fig. 5).

The pig carotid media F_0 is 3.7×10^5 N/m^2 cell cross-sectional area (Murphy et al. 1974). This value exceeds that of skeletal muscle (Close, 1972) and is accomplished with only about one-fourth as much myosin (but about twice as much actin) (Murphy et al., 1974). Our experiments reported here and elsewhere (Driska and Murphy, 1978) have led us to reject the hypothesis that high force development in the pig carotid is due to parallel linkage of cells anatomically in series. The available data indicate that individual smooth muscle cells are capable of developing high forces. Likely explanations for the high force development with few potential cross-bridges include (*a*) possible differences in the kinetics of cross-bridge cycling, or (*b*) a filament lattice geometry which places a high fraction of the cross-bridges in parallel within the cell (Ashton et al., 1975; Mrwa et al., 1976; Murphy, 1976; Rosenbluth, 1965).

We thank Dr. Brian R. Duling for the use of video recording microscopy apparatus, Dr. Howard Kutchai for the sucrose space measurements, and Dr. Donald Ramirez for advice and the computer programs used in the statistical analysis of cell length data.

This work was supported by National Institutes of Health grants HL 14547, PO1 HL 19242, and HL 12792.

Received for publication 8 April 1978 and in revised form 13 July 1978.

REFERENCES

ARBORGH, B., P. BELL, U. BRUNK, and V. P. COLLINS. 1976. The osmotic effect of glutaraldehyde during fixation. A transmission electron microscopy, scanning electron microscopy and cytochemical study. *J. Ultrastruct. Res.* **56**:339.

ASHTON, F. T., A. V. SOMLYO, and A. P. SOMLYO. 1975. The contractile apparatus of vascular smooth muscle: intermediate high voltage stereo electron microscopy. *J. Mol. Biol.* **98**:17.

BADER, H. 1963. The anatomy and physiology of the vascular wall. *Handb. Physiol.* **2**(Sect. 2, Circulation): 865.

BAGBY, R. M. 1974. Time course of isotonic contraction in single cells and muscle strips from *Bufo marinus* stomach. *Am. J. Physiol.* **227**:789.

BURTON, A. C. 1954. Relation of structure to function of the tissues of the wall of blood vessels. *Physiol. Rev.* **34**:619.

BURY, K. V. 1975. Statistical Models in Applied Science. John Wiley & Sons, Inc., New York. 300–301.

CLOSE, R. I. 1972. Dynamic properties of mammalian skeletal muscles. *Physiol. Rev.* **52**:129.

COOKE, P. H., and F. S. FAY. 1972. Correlation between fiber length, ultrastructure, and the length-tension relationship of mammalian smooth muscle. *J. Cell Biol.* **52**:105.

DRISKA, S. P., and R. A. MURPHY. 1978. An estimate of cellular force generation in an arterial smooth muscle with a high actin:myosin ratio. *Blood Vessels.* **15**:26.

FAY, F. S. 1977. Mechanics of single isolated smooth muscle cells. *In* Excitation-Contraction Coupling in Smooth Muscle. R. Casteels, T. Godfraind, and J. C. Ruegg, editors, Elsevier/North-Holland, Amsterdam. 433.

FAY, F. S., and J. J. SINGER. 1977. Characteristics of response of isolated smooth muscle cells to cholinergic drugs. *Am. J. Physiol.* **232**:C144.

GABELLA, G. 1976. The force generated by a visceral smooth muscle. *J. Physiol. (Lond.).* **263**:199.

GORCZYNSKI, R. J. 1976. The microcirculatory basis of functional hyperemia in striated muscle. Ph.D. Thesis, University of Virginia, Charlottesville, Va. University Microfilms, Ann Arbor, Mich. 201–203.

GROSS, A. J., and V. A. CLARK. 1975. Survival Distributions: Reliability Applications in the Biomedical Sciences. John Wiley & Sons, Inc. New York. 228.

HALPERN, W., M. J. MULVANY, and D. M. WARSHAW. 1978. Mechanical properties of smooth muscle cells in the walls of arterial resistance vessels. *J. Physiol. (Lond.)* **275**:85.

HERLIHY, J. T., and R. A. MURPHY. 1973. Length-tension relationship of smooth muscle of the hog carotid artery. *Circ. Res.* **33**:275.

HERLIHY, J. T., and R. A. MURPHY. 1974. Force-velocity and series elastic characteristics of smooth muscle from the hog carotid artery. *Circ. Res.* **34**:461.

HUXLEY, A. F. 1957. Muscle structure and theories of contraction. *Prog. Biophys. Biophys. Chem.* **7**:255.

JEWELL, B. R., and D. R. WILKIE. 1958. An analysis of the mechanical components in frog's striated muscle. *J. Physiol. (Lond.)* **143**:515.

MEISS, R. A. 1978. Dynamic stiffness of rabbit mesotubarium smooth muscle: effect of isometric length. *Am. J. Physiol.* **234**:C14.

MRWA, U., R. J. PAUL, V. A. W. KREYE, and J. C. RÜEGG. 1976. The contractile mechanism of vascular smooth muscle. *In* Smooth Muscle Pharmacology and Physiology. M. Worcel and G. Vassort, editors. Institut National de la Sante et de la Recherche Médicale. Paris. 319.

MURPHY, R. A. 1976. Contractile system function in mammalian smooth muscle. *Blood Vessels.* **13**:1.

MURPHY, R. A., S. P. DRISKA, and D. M. COHEN. 1977. Variations in actin to myosin ratios and cellular force generation in vertebrate smooth muscles. *In* Excitation-Contraction Coupling in Smooth Muscle. R. Casteels, T. Godfraind, and J. C. Rüegg, editors. Elsevier/North-Holland, Amsterdam. 417.

MURPHY, R. A., J. T. HERLIHY, and J. MEGERMAN. 1974. Force-generating capacity and contractile protein content of arterial smooth muscle. *J. Gen. Physiol.* **64**:691.

ROSENBLUTH, J. 1965. Smooth muscle: an ultrastructural basis for the dynamics of its contraction. *Science (Wash. D.C.).* **148**:1337.

SMALL, J. V. 1977. Studies on isolated smooth muscle cells: the contractile apparatus. *J. Cell Sci.* **24**:327.

UVELIUS, B. 1976. Isometric and isotonic length-tension relations and variations in cell length in longitudinal smooth muscles from rabbit urinary bladder. *Acta Physiol. Scand.* **97**:1.